Scanning Microscopy

Volume 3 | Number 3 Article 1

9-27-1989

Simultaneous Micro-Characterization of the Superconducting and Structural Properties of High-Tc Superconducting Films

R. P. Huebener
Universität Tübingen

R. Gross
Universität Tübingen

Scanning Microscopy, Vol. 3, No. 3, 1989 (Pages 703-710)
Scanning Microscopy International, Chicago (AMF O'Hare), IL 60666 USA

0891-7035/89$3.00+.00

SIMULTANEOUS MICRO-CHARACTERIZATION OF THE SUPERCONDUCTING AND STRUCTURAL PROPERTIES OF HIGH-T_c SUPERCONDUCTING FILMS

R. P. Huebener* and R. Gross

Physikalisches Institut, Lehrstuhl Experimentalphysik II
Universität Tübingen, D-7400 Tübingen, Fed. Rep. Germany

(Received for publication April 20, 1989, and in revised form September 27, 1989)

Abstract

Important information on the local values of the critical temperature and the critical current density in high-T_c superconducting films is obtained by low-temperature scanning electron microscopy (LTSEM). The imaging principle of LTSEM is based on the local beam-induced heating effect and the detection of a voltage response signal in the current-biased specimen film. During the scanning process the sample is mounted on a low-temperature stage the temperature of which is electronically stabilized at some specific value in the range of interest. The local superconducting quantities measured by LTSEM can be correlated with the microstructure of the specimen film investigated by standard techniques. Recently we have studied polycrystalline and epitaxial YBaCuO films on various substrates, and the results are summarized. The spatial resolution of LTSEM has been found to approach 1 μm.

KEY WORDS: High-T_c superconducting films, low temperature scanning electron microscopy, critical temperature, critical current density, cold stage, YBaCuO, electron beam scanning

*Address for correspondence:
R. P. Huebener, Physikalisches Institut, Lehrstuhl Experimentalphysik II, Universität Tübingen, D-7400 Tübingen, Fed. Rep. Germany
Phone No. (07071) 296315

Introduction

Following the recent discovery of the Cu-oxide based high-T_c superconductors, a large amount of research and development is being concentrated at present on these superconducting materials in many laboratories. From this work it has become clear already that the new high-T_c superconductors show much more complicated behavior than most of the "classical" superconducting materials. Mainly these complications are due to the following facts: (1) There exist several structural phases for each class of materials; (2) The superconducting properties are highly sensitive to the exact stoichiometry and in particular to the oxygen concentration; (3) Strong anisotropy; (4) Possibility of twinning due to the reversal of the a- and b-axes; (5) Strong influence of grain boundaries; (6) Extreme sensitivity to imperfections because of the small value of the superconducting coherence length. In the field of high-temperature superconductivity the preparation of thin films represents a particularly important direction because of many possible electronic applications based on thin-film configurations. Here the successful fabrication of high-T_c films showing critical current densities in excess of 10^6 A/cm^2 at 77 K looks highly encouraging [2,14,15].

For the electric characterization of high-T_c superconducting films one usually measures the electric resistivity as a function of temperature, the main objective being the determination of the critical temperature T_c at which the resistivity abruptly drops to zero. During these measurements the electric bias current through the sample is often made infinitesimally small. Whereas such measurements immediately can confirm the presence of superconductivity, they do not provide any information regarding the relative amount of the superconducting phase in the sample (except for the question of whether or not the two voltage probes are linked by a continuous superconducting path). Additional important information on the superconducting sample properties is obtained by measuring the critical current density and its temperature dependence. In addition to the existence of a superconducting path through the specimen at the operating temperature, the latter measurement probes its current carrying capacity

and, therefore, gives a first hint regarding the sample fraction occupied by the superconducting phase. In polycrystalline materials the critical current has been found to be limited by grain boundaries [2]. Measurements of the magnetic susceptibility and of its temperature dependence also yield useful information on the superconducting sample fraction.

It is important to note that both the electric resistivity and the critical current density obtained from transport measurements as well as the magnetic susceptibility represent global properties. However, in view of the complicated behavior of the high-T_c materials mentioned above, one must expect strongly inhomogeneous properties of the high-T_c films. Whereas such inhomogeneities are expected in particular for polycrystalline films, epitaxial films can also display inhomogeneous behavior due to various reasons. In the former case we have to deal with differences in the composition and orientation of the grains, with the grain boundaries, and possibly with nonsuperconducting inclusions. In the latter case we can encounter spatial variations in the film thickness and nonuniform growth properties. Since superconducting epitaxial films with a relatively high critical current density can now be prepared with a thickness as small as only a few ten nm, such films become sensitive also to small spatial nonuniformities of the substrate surface. A general problem can arise due to possible damage of the area near the film edges caused by the microfabrication process (photolithography, laser ablation, various etching procedures, etc.). These arguments clearly show that a technique for investigating the superconducting thin film properties with high spatial resolution instead of only global measurements becomes necessary in order to obtain a good understanding of the electronic film behavior. A technique accomplishing this task is now available, namely low temperature scanning electron microscopy (LTSEM). The principle of this technique is simple. The specimen film is scanned with the electron beam of a scanning electron microscope while it is cooled to the temperature range where it becomes superconducting. Simultaneously, an electric bias current is applied to the film, and the beam-induced resistive voltage change $\delta V(x,y)$ is recorded as a function of the coordinate point (x,y) of the electron beam focus on the film surface.

By means of LTSEM one can determine the local values of the critical temperature $T_c(x,y)$ and of the critical current density $j_c(x,y)$ of high-T_c superconducting films with a spatial resolution approaching at least 1 μm. In this way the superconducting properties $T_c(x,y)$ and $j_c(x,y)$ can be imaged two-dimensionally as a function of the coordinate point (x,y) on the film. Following such investigations, the results can be correlated with the local microstructure of the superconducting films studied by the standard techniques for microstructure and surface analysis. A large part of the latter standard methods can be employed using the same scanning electron microscope in a different mode of operation than during LTSEM.

In this paper we outline the essential ideas of LTSEM for studying high-T_c superconducting films and illustrate this new analytic method with characteristic examples.

Principles of LTSEM

The experimental arrangements one needs for performing LTSEM studies on high-T_c superconducting films are outlined schematically in Fig. 1. The substrate carrying the specimen film is mounted on a temperature controlled cold-stage such that the sample temperature can be kept at any desired value between, say, 4.2 K and room temperature.

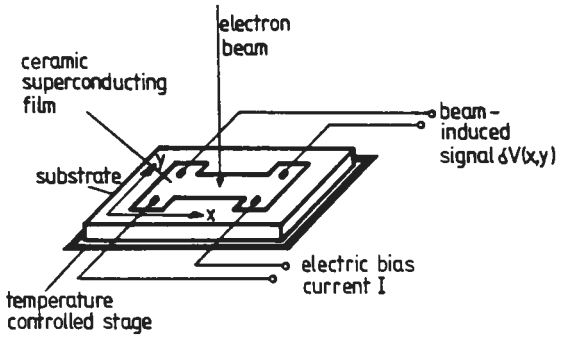

Fig. 1: Principle of LTSEM applied to ceramic superconducting films.

For the temperature range below 77 K liquid helium serves as the cooling medium, whereas for temperatures between 77 K and room temperature liquid nitrogen can be used. Electronic temperature control of the cold stage is achieved by means of an attached electric heater (wound bifilarly) and thermometer. In order to ensure that the temperature of the sample and the temperature of the cold stage (measured by the thermometer)are nearly the same, good thermal coupling between the specimen film and the cold stage is required. On the other hand, the thermal coupling between the cold stage and the cooling medium must be carefully adjusted in order to reach operating temperatures of the cold stage sufficiently above the boiling point of the cooling medium (by means of the electric heater) if necessary. The essential features of the cold stage are shown schematically in Fig.2. During the LTSEM experiments the complete cold stage is inserted into the sample chamber of the scanning electron microscope, such that the specimen film can be scanned directly with the electron beam while its temperature is kept at a specified low value. Electric current and voltage leads are attached to the specimen. While an electric bias current is passed through the sample, the sample surface is scanned by the electron beam and the beam-induced resistive voltage change $\delta V(x,y)$ is recorded as a function of the coordinate point (x,y) of the electron beam focus on the film surface.

A more detailed description of the cold stage we have used for studying high-T_c superconducting films can be found elsewhere [6]. The applications

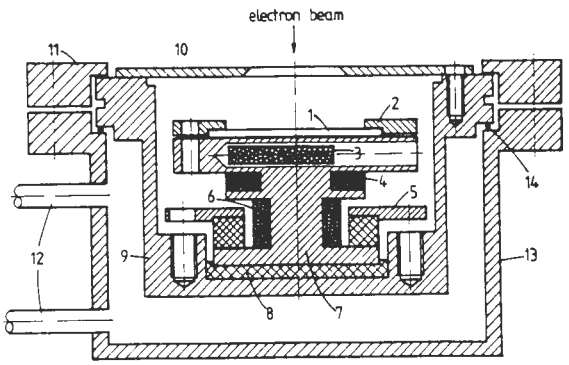

Fig. 2: Cross-section of the low-temperature stage. 1 - substrate with specimen film, 2 - clamping ring, 3 - temperature sensor, 4 - magnetic field coil, 5 - clamping ring, 6 - bifilarly wound heater, 7 - copper cold finger, 8 - thermal coupling disk, 9 - lid of tank for cryo-liquid (LHe, LN_2), 10 - thermal shield, 11 - clamping ring, 12 - tubes for cryo-liquid, 13 - small tank for cryo-liquid, 14 - indium seal.

of LTSEM to high-temperature superconductors discussed in the following represent an extension of our earlier work dealing with the classical superconductors and superconducting tunnel junctions [1,11]. A summary of all earlier work based on LTSEM before the advent of the high-T_c superconductors can be found in a recent review [10].

Beam Induced Voltage Signal

The electron beam irradiation of the high-T_c superconducting film results mainly in a local heating effect at the coordinate point of the beam focus on the sample. The interaction of the beam electrons of typical energies between 10 and 30 keV with a superconducting crystal is well understood [1,3,13]. In a characteristic time of typically less than 10^{-11} sec, the beam electrons are stopped in the irradiated crystal by Coulomb interaction. The penetration depth of the beam electrons depends on the electron energy and on the average atomic number and the density of the irradiated material. For the high-T_c superconductor YBaCuO the penetration depth of 30 keV electrons is, for example, about 2.3 µm. During their stopping and thermalization process the beam electrons generate different types of excitations such as quasiparticles and phonons in the superconductor. The spatial and temporal structure of the non-equilibrium state generated by the localized electron beam irradiation is determined by the relaxation and diffusion processes of the excitations and can be calculated by solving their coupled diffusion equations [3].

Usually, a description of the electron beam induced perturbation as a local heating effect represents an adequate approximation, since a thermal quasi-equilibrium among the different excitations at an elevated temperature is established on a sufficiently short time scale. In this case the resulting nonequilibrium state can simply be characterized by an elevated effective temperature T*. A detailed analysis of this situation for high-T_c films based on the thermal diffusion equation has been published elsewhere [8]. The main results are the following, again taking YBaCuO as an example. For an operating temperature of 90 K (i.e., near the critical temperature T_c of YBaCuO) and for an electron beam power in the range of 1 - 10 µW, the beam-induced local temperature increment δT amounts to about 0.1 - 1 K. The spatial resolution obtained for this application of LTSEM is limited by the characteristic decay length of the thermal perturbation, and a resolution limit of 1 µm or smaller can be expected. It appears that relatively low beam energies around, say, 5 keV are favorable for obtaining maximum spatial resolution.

Having convinced ourselves that the sample perturbation due to the electron beam irradiation is mainly a local heating effect yielding a local temperature increment δT, the principles for imaging the local superconducting properties $T_c(x,y)$ and $j_c(x,y)$ of high-T_c films are quickly established. Turning first to the critical temperature $T_c(x,y)$, we note that the electric resistivity $\rho(T)$ of a superconductor plotted versus temperature yields a curve with a steep slope near T_c, as shown in Fig. 3 at the top. Below T_c the resistivity is zero, whereas above T_c the slope of the function $\rho(T)$ is much smaller than near T_c.

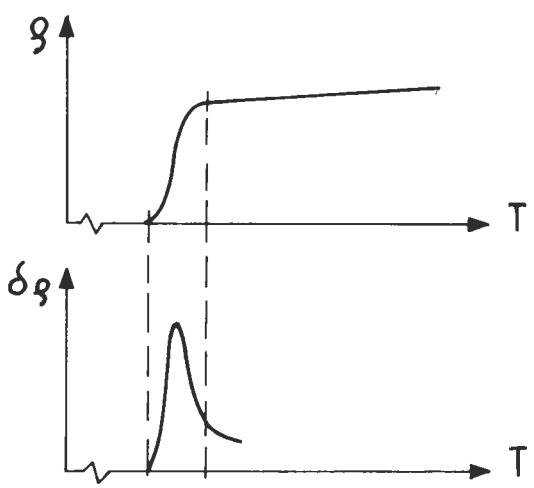

Fig. 3: Electric resistivity ρ (top) and beam-induced resistivity change $\delta\rho$ (bottom) versus temperature T.

We see that the beam-induced local temperature increment results in a resistivity change $\delta\rho(T)$ which strongly depends on the operating temperature of the experiment. If the temperature increment δT is sufficiently small, the curve $\delta\rho(T)$ shows a sharp maximum near the critical temperature T_c where the steepest slope is reached by the function $\rho(T)$. This is indicated in Fig. 3 at the bottom. Clearly, if a constant bias current is

passed through the sample, a voltage signal $\delta V(T)$ is produced which depends upon the operating temperature and has a sharp maximum near T_c, similar to the $\delta\rho(T)$ curve. In this way the maximum of the voltage signal $\delta V(T)$ nearly images the critical temperature T_c where the $\rho(T)$ curve displays the steepest slope. A direct experimental proof of this principle has been demonstrated recently [8]. Of course, the voltage signal $\delta V(T)$ increases with increasing fraction of the sample cross section perturbed by the electron beam. Therefore, the width of the specimen film (measured perpendicular to the flow direction of the bias current) must be kept small in order to obtain a reasonably strong response signal $\delta V(T)$. The maximum allowed values for the sample width lie in the range 100 - 200 µm. Such specimen films can easily be prepared using standard microfabrication procedures.

So far we have assumed that the sample is completely homogeneous. Next we assume that the critical temperature T_c varies throughout the sample. For simplicity we restrict ourselves to the one-dimenisonal case where T_c varies only along the x-direction of the current flow and remains constant in the perpendicular directions. As an example we take three regions with different T_c values, as shown by the $\rho(T)$ curves in Fig. 4 at the top.

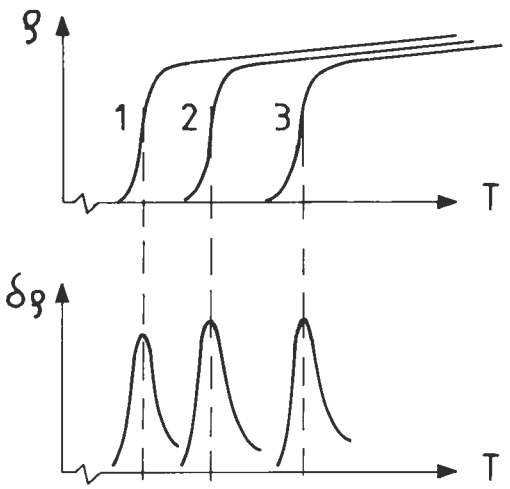

Fig. 4: Electric resistivity ρ (top) and beam-induced resistivity change $\delta\rho$ (bottom) versus temperature T for three regions with different transition temperature.

The corresponding curves for the beam-induced resistivity change $\delta\rho(T)$ are shown in Fig. 4 at the bottom. From the latter curves we see that in a current biased sample a maximum voltage signal arises in those regions where the critical temperature is close to the temperature at which the scanning process is performed. In this way the T_c variation throughout the sample can be imaged by means of the voltage signal $\delta V(x)$ recorded at different temperatures. Of course, for spatially resolving the regions with the different T_c-values, the beam-induced local temperature increment δT must be small compared to the total spatial spread ΔT_c of the T_c-values:

$$\delta T << \Delta T_c \qquad (1)$$

The ideas outlined above can be extended to the one-dimensional case where T_c varies only in y-direction perpendicular to the current flow, and to the two-dimensional case where T_c varies over the plane of the film. Further, the current signals δI obtained for voltage-biased operation can be calculated. A detailed discussion of these generalizations has been given elsewhere [12].

Turning next to the scheme for imaging the spatial distribution of the critical current density $j_c(x,y)$, we note that the electric resistivity $\rho(I)$ of a superconductor plotted versus the current I at constant temperature $T < T_c$ yields a curve with a steep slope above the critical current I_c, as shown in Fig. 5 at the top.

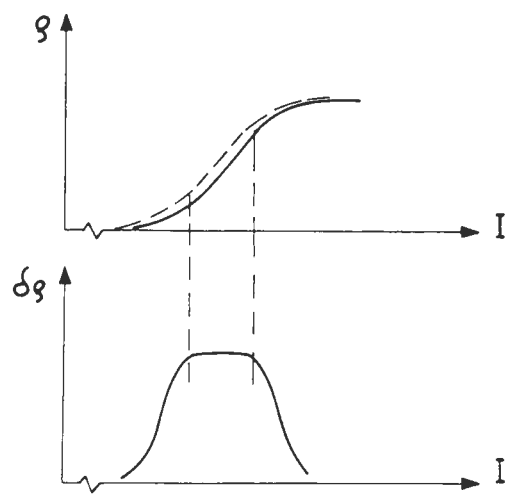

Fig. 5: Electric resistivity ρ (top) and beam-induced resistivity change $\delta\rho$ (bottom) versus current I.

The critical current I_c is defined as the smallest current value at which a resistive voltage can be detected. (For practical reasons I_c is often specified in terms of a finite voltage threshold of, say, 1 µV). For $I < I_c$ the superconducting state with zero resistivity is attained. In the current-induced resistive state for $I > I_c$ the resistivity increases strongly with increasing current, displaying large deviations from Ohm's law. A detailed discussion of this non-ohmic behavior can be found elsewhere [9]. For currents sufficiently above I_c the superconductor reaches the normal state, and Ohm's law prevails again, the resistivity becoming independent of the current. Due to the beam-induced local temperature

increment δT the $\rho(I)$ curve is shifted slightly to smaller currents, as indicated by the dashed line in Fig. 5 at the top. We see that the beam irradiation results in a resistivity change $\delta\rho(I)$ which strongly depends on the bias current. Again, if the temperature increment δT is sufficiently small, the curve $\delta\rho(I)$ displays a sharp maximum near the current where the steepest slope is reached in the function $\rho(I)$. This is indicated in Fig. 5 at the bottom. For a constant bias current the beam irradiation produces a voltage signal $\delta V(I)$ which depends on the current and has a sharp maximum slightly above I_c, similar to the $\delta\rho(I)$ curve. The onset of the voltage signal $\delta V(I)$ images the critical current I_c at which resistance starts to appear in the voltage-current characteristic.

Our further discussion can proceed analogous to the arguments presented above in our treatment of the process for imaging the spatial distribution of the critical temperature $T_c(x,y)$. Considering now the variations of the critical current density j_c throughout the sample, for simplicity we look first at the one-dimensional case where j_c varies only along the x-direction of the current flow. As an example we take again three regions with different I_c values as shown by the $\rho(I)$ curves in Fig. 6 at the top. The corresponding curves for the beam-induced resistivity change $\delta\rho(I)$ are shown in Fig. 6 at the bottom. From the latter curves we see that the onset of the voltage signal $\delta V(I)$ images the regions which just become resistive at the particular values of the bias current

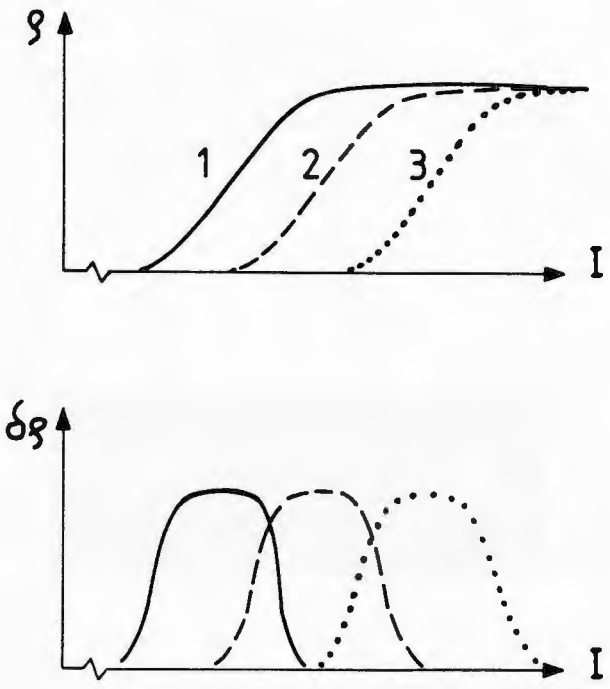

Fig. 6: Electric resistivity ρ (top) and beam-induced resistivity change $\delta\rho$ (bottom) versus current I for three regions with different critical currents.

and the temperature adopted during the scanning process. The experimental procedure for this imaging process is then as follows. At a fixed temperature $T < T_c$, starting from a small value the bias current is increased in small steps. After each current step the sample is scanned with the electron beam. A nonzero beam-induced voltage signal $\delta V(x)$ first appears at the x-coordinate of the region with the smallest local value $I_c(x)$ of the critical current. As the bias current is stepwise increased, more and more regions with higher values of the critical current produce a voltage signal. In this way the spatially resolved values $I_c(x)$ can be recorded. Of course, for spatially resolving the regions with the different I_c-values, the beam-induced reduction $|\delta I_c|$ (indicated by the dashed curve in Fig. 5 at the top) must be small compared to the total spatial spread ΔI_c of the different I_c-values:

$$|\delta I_c| \ll \Delta I_c \quad . \tag{2}$$

The ideas outlined above can be extended to the two-dimensional case where the local critical current density $j_c(x,y)$ is a function of both the x- and y-coordinate in the plane of the film, and a detailed discussion can be found elsewhere [8,12]. As a result one finds that the two-dimensional distribution $j_c(x,y)$ of the local critical current density can be imaged by means of the voltage signal $\delta V(x,y)$.

Finally, we emphasize again that the principles for imaging the distribution $T_c(x,y)$ at constant (infinitesimal) bias current and the distribution $j_c(x,y)$ at constant temperature are highly analogous, both principles being based on the steep slope of the curves $\rho(T)$ and $\rho(I)$ in the critical regions near $T = T_c$ and $I = I_c$, respectively, (see the top parts of Fig. 3 and Fig. 5). Of course, this highly nonlinear form of the curves $\rho(T)$ and $\rho(I)$ is favorable for generating a voltage signal $\delta V(x,y)$ displaying sharp spatial structures.

YBaCuO Films Studied by LTSEM

The validity of the concepts outlined above has been demonstrated recently in experiments performed with superconducting YBaCuO films [4,5,7,8]. The film thickness of these studies ranged around 1 - 2 μm. The energy of the beam electrons and the beam power were typically 25 keV, and 10 μW, respectively. In YBaCuO the penetration range of 25 kV electrons is about 1.8 μm. Hence, for the samples investigated the beam energy was dissipated predominantly in the YBaCuO films and not in the underlying substrate material. The spatial resolution obtained for the two-dimensional imaging of the distribution of the critical current density $j(x,y)$ was about 1 - 2 μm. Such a value is expected from a thermal analysis of the beam-induced local heating effect in the specimen [8].

As a typical example for the beam-induced voltage signal $\delta V(x,y)$ we show in Fig. 7 a series of line scans carried out along the middle of a polycrystalline YBaCuO film parallel to the flow

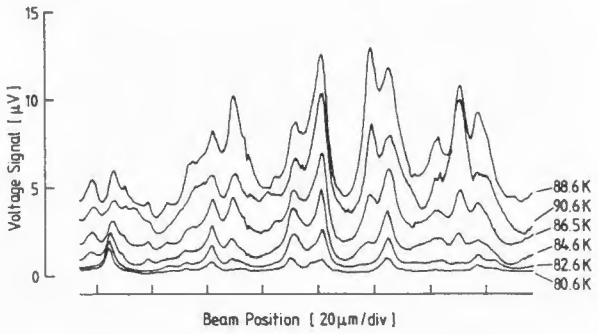

Fig. 7: Beam-induced voltage signal $\delta V(x)$ for a series of line scans carried out along the middle of a polycrystalline YBaCuO-film (width = 30 μm; thickness = 1.1 μm) parallel to the average current direction at constant bias current I = 10 μA and different temperatures as shown on the right. Beam parameters: 25 kV, 2 nA, 10 kHz modulation.

direction of the bias current (x-direction). The superconducting bridge was 30 μm wide and 1.1 μm thick. The bias current was 10 μA, and the sample temperature was varied between 80.6 and 90.6 K. The electron beam was modulated at 10 kHz, and the voltage signal $\delta V(x,y)$ was measured with a lock-in detector. In Fig. 7 the signal $\delta V(x)$ is plotted as a function of the x-coordinate at constant value of the y-coordinate. We see that for the lowest temperature a finite signal $\delta V(x)$ is detected only at a few beam positions along the scanning line. It is only in these sample regions where nonzero resistance appears along the scanning line during the beam irradiation, whereas all other regions still remain superconducting. Apparently, for temperatures higher than 82 K a nonzero voltage signal is observed along the whole length of the film shown. The signal $\delta V(x)$ increases with increasing temperature and passes through a maximum expected near the temperature where the temperature derivative $\partial\rho/\partial T$ of the resistivity reaches its peak value. For temperatures above 93 K the spatial variation of the observed voltage signal $\delta V(x)$ disappeared. From recordings such as shown in Fig. 7, the spatial variation of the critical temperature $T_c(x,y)$ at the selected value of the bias current can be investigated. From the fine structure of the curves in Fig. 7, we see that a spatial resolution of 1 - 2 μm can be achieved.

Recordings displayed in y-modulation such as shown in Fig. 7, where the beam-induced signal is plotted versus the running coordinate of the line scan, are favorable for performing a quantitative analysis of the results. On the other hand, useful overall information about the two-dimensional variations of the sample behavior is obtained from images generated by brightness modulation. In this case, the beam-induced signal serves for controlling the brightness on the video screen of the SEM. Usually, bright regions correspond to large values of the signal. Such a two-dimensional image obtained by brightness modulation is shown in Fig. 8. The sample is a polycrystalline YBaCuO film of 2.5 μm thickness and 42 μm width. The superconducting bridge extends horizontally. Its edges are marked with the white lines at the top and bottom, indicating the much wider film sections at the left and right. In this sample, zero resistance was reached at the temperature T_c^0 = 80 K. The image was generated at 83 K with 40 μA bias current. As seen from Fig. 8, the superconducting film is highly inhomogeneous. Whereas most of the constricted part of the bridge produces only a small voltage signal, this signal is considerably larger in the outer regions. Apparently, the critical temperature in these outer regions is slightly smaller than in the middle part of the bridge. The bottom part of Fig. 8 shows the voltage signal in y-modulation for a line scan. The location of this line scan is marked by the horizontal white line in the center of the image at the top.

In Fig. 9 we show results obtained with an epitaxial YBaCuO film of 12 μm width and 0.5 μm thickness. The film extends horizontally, and the location of the upper and lower boundary is marked by the black arrows. The voltage image was taken at 79.6 K with a bias current of 21.2 mA. In the bright regions the bias current exceeds the critical current of the superconducting line. Again, strongly inhomogeneous behavior is observed by means of LTSEM. Whereas at the current density $3.5 \cdot 10^5$ A/cm^2 resistance appears in the sample locally (bright regions) other parts still remain superconducting (dark regions) indicating a larger value of the local critical current density. The example shown in Fig. 9 demonstrates how the spatial distribution of the critical current density $j_c(x,y)$ in high-T_c superconducting films can be imaged.

Concluding Remarks

Our experiments have shown that LTSEM represents a powerful method for investigating the two-dimensional variation of the characteristic properties of superconducting high-T_c films such as the critical temperature and the critical current density. So far we have achieved a spatial resolution of 1 - 2 μm. The method has some similarity with the electron beam testing principles which are widely used today for studying the functional behavior of the integrated circuit configurations on semiconductor chips. Similar to the role of electron beam testing in the semiconductor technology, LTSEM is expected to play an important role both in fundamental studies and in the functional testing and the quality control of microelectronic devices based on superconducting high-T_c films. Among such applications of superconducting high-T_c films intra-chip and inter-chip connecting lines, microwave devices, magnetic and electric sensors, and high-Q resonators appear promising at present.

Of course, the spatially resolved study of the superconducting properties must be correlated with the local microstructure and chemical composition of the sample films as obtained from the standard techniques available today. In this way, the directions for optimizing the film properties can be found. In addition to the preparation of thin films of high quality, microfabrication of the required geometric structures represents an important step which must be optimized also. The various microfabrication techniques (photo-lithography,

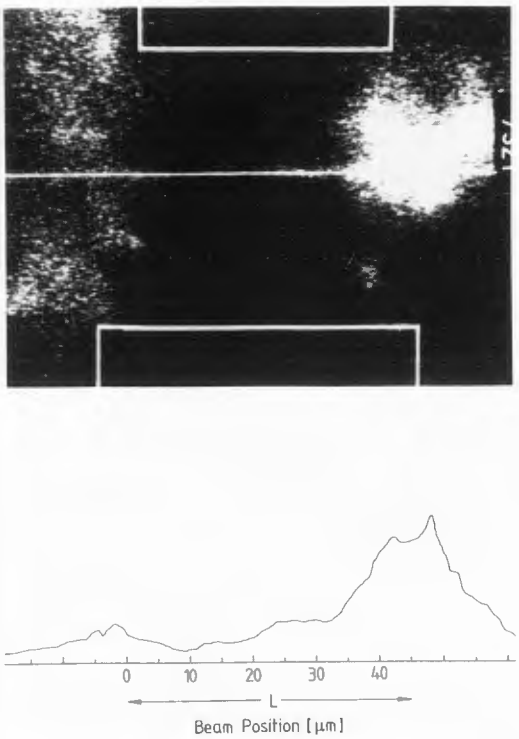

Fig.8: Voltage image $\delta V(x,y)$(top) and voltage signal $\delta V(x,y_0)$for a line scan in "y-modulation" of a polycrystalline YBaCuO-film of 2.5 µm thickness and 42 µm width taken at 83 K and 40 µA bias current. At the top the location of the line scan is marked by the horizontal white line in the center. The bridge extends horizontally, and its edges are indicated by the white lines at the top and bottom. Beam parameters: 26 kV, 560 nA, 10 kHz modulation.

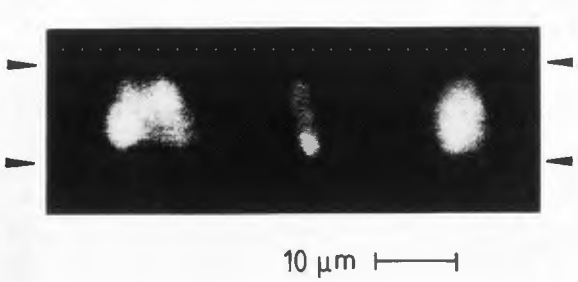

Fig. 9: Voltage image $\delta V(x,y)$ for a superconducting line of 12 µm width patterned in an epitaxial YBaCuO-film by laser ablation. Temperature = 79.6 K, bias current = 21.2 mA. The line extends horizontally, and the location of the upper and lower edge is marked by the black arrows. Beam parameters: 26 kV, 2 nA, 10 kHz modulation.

reactive ion etching, chemical etching, laser ablation, etc.) can have different effects on the superconducting film properties, in particular close to the film edges. Here spatially resolved tests for quality control will become crucial, and LTSEM is expected to play an important role.

Acknowledgement

Financial support of this work by the Bundesministerium für Forschung und Technologie (Project No. 13N5482) is gratefully acknowledged.

References

[1] Clem JR, Huebener RP (1980) Applications of Low-Temperature Scanning Electron Microscopy. J. Appl. Phys. 51, 2764-2773.

[2] Dimos D, Chaudhari P, Mannhart J, LeGoues FK (1988) Orientation Dependence of Grain-Boundary Critical Currents in $YBa_2Cu_3O_{7-\delta}$ Bicrystals. Phys. Rev. Lett. 61, 219-222.

[3] Gross R, Koyanagi M (1985) Effect of Electron-Beam Irradiation on Superconducting Films. J. Low Temp. Phys. 60, 277-295.

[4] Gross R, Hartmann M, Hipler K, Huebener RP, Kober F, Koelle D (1988) Spatial Resolution Limit For The Investigation of High-T_c Films By Low Temperature Scanning Electron Microscopy. Proceedings of the Applied Superconductivity Conference, San Francisco, CA. USA. IEEE Trans. Magnetics 25, No. 2, 2250-2253.

[5] Gross R, Bosch J, Huebener RP, Mannhart J, Tsuei CC, Scheuermann M, Oprysko MM, Chi CC (1988) Spatially resolved observation of the critical current in high-T_c superconducting films. Nature 332, 818-819.

[6] Gross R, Bosch J, Wener HG, Fischer J, Huebener RP (1989) Temperature Stabilized Sample Stage for the Investigation of High-T_c Superconductors by Scanning Electron Microscopy. Cryogenics 29, 716-719.

[7] Gross R, Hipler K, Mannhart J, Huebener RP, Chaudhari P, Dimos D, Tsuei CC, Schubert J, Poppe U (1989) Spatial Imaging of the Critical Current Density in Epitaxial $Y_1Ba_2Cu_3O_7$-Films. in press.

[8] Hartmann M, Hipler K, Koelle D, Kober F, Bernhardt K, Sermet T, Gross R, Huebener RP (1989) Characterization of Superconducting YBaCuO-Films By Low Temperature Scanning Electron Microscopy. Z. Phys. B - Cond. Matter 75, 423-432.

[9] Huebener RP (1979) Magnetic Flux Structures in Superconductors. Springer-Verlag, Berlin.

[10] Huebener RP (1988) Scanning Electron Microscopy at Very Low Temperatures. In: Advances in Electronics and Electron Physics, PW Hawkes (ed), Academic Press, New York, Vol.70, 1-78.

[11] Huebener RP, Seifert H (1984) Applications of Low-Temperature Scanning Electron Microscopy. Scanning Electron Microsc. 1984; III: 1053-1963.

[12] Huebener RP, Gross R, Bosch J (1988) Low-Temperature Scanning Electron Microscopy for Studying Inhomogeneities in Thin-Film High-T_c Superconductors. Z. Phys. B - Cond. Matter 70, 425-430.

[13] Reimer LW (1985) Scanning Electron Microscopy. Springer-Verlag, Berlin.

[14] Roas B, Schultz L, Endres G (1988) Epitaxial growth of $YBa_2Cu_3O_{7-x}$ thin films by a laser evaporation process. Appl. Phys. Lett. 53, 1557-1559.

[15] Xi XX, Linker G, Meyer O, Nold E, Obst B, Ratzel F, Smithey R, Strehlau B, Weschenfelder F, Geerk J (1989) Superconducting and Structural Properties of YBaCuO Thin Films Deposited by Inverted Cylindrical Magnetron Sputtering. Z. Phys. B - Cond. Matter 74, 13-19.

Discussion with Reviewers

D. Koehler: Do your techniques provide information only of the irradiated specimen area or can the signal be influenced by distant specimen regions?
Authors: In the applications discussed in this paper,the signal is generated only by the local region which is thermally perturbed by the beam. However, in some applications such as the imaging of the pair current distribution in superconducting tunnel junctions,a nonlocal contribution to the signal is possible since the pair tunneling process is described by a wave function.